ChemComm

Cite this: *Chem. Commun.*, 2012, **48**, 3391–3393

www.rsc.org/chemcomm

COMMUNICATION

Enhancement of the electrocatalytic activity of Pt nanoparticles in oxygen reduction by chlorophenyl functionalization†

Zhi-You Zhou,[ab] Xiongwu Kang,[a] Yang Song[a] and Shaowei Chen*[a]

Received 20th December 2011, Accepted 4th February 2012
DOI: 10.1039/c2cc17945h

Chlorophenyl-stabilized platinum nanoparticles (1.85 nm) exhibited electrocatalytic activity for oxygen reduction up to 3 times higher than that of commercial Pt/C catalysts. Similar enhancement was observed with naked Pt/C functionalized by the same chlorophenyl fragments, suggesting the important role of organic capping ligands in the manipulation of nanoparticle electrocatalytic performance.

Proton exchange membrane fuel cells are a promising clean energy source. However, the commercialization is seriously impeded by the poor performance of cathodic catalysts in oxygen reduction reactions (ORR). The sluggish kinetics of ORR decreases the thermal efficiency by as much as 30–40% even with the use of state-of-the-art Pt catalysts.[1] The Pt catalysts are usually dispersed as fine particles on carbon black (Pt/C) to reduce Pt loading and to enhance surface accessibility. However, the area-specific ORR activity of Pt nanoparticles has been found to decrease with decreasing particle size.[2,3] As a result, the mass activity of Pt begins to decline when the size is smaller than 3 nm (which is therefore adopted as the ''threshold'' size for state-of-the-art Pt/C catalysts).[2] To further improve the ORR activity, substantial efforts have been devoted to the manipulation of the composition and morphology of Pt-based catalysts, such as Pt-monolayer catalysts,[4,5] Pt–M (M = Fe, Co, Ni, Pd, etc) alloy catalysts,[6–8] and shape-controlled nanocrystals.[9,10]

Recently, there has emerged another effective strategy where the electrocatalytic performance may be tuned by the deliberate chemical functionalization of noble metal surfaces with specific molecules/ions.[11–14] Of these, aryl-stabilized metal nanoparticles through M–C covalent bonds have received great interest.[15–17] The grafting of aryl groups onto the metal surfaces is effected by the active aryl radicals (Ar$^{\bullet}$) that are generated from the reduction of diazonium precursors.[18] Herein, we prepared chlorophenyl-functionalized Pt (Pt–ArCl) nanoparticles (core dia. 1.85 ± 0.28 nm), and observed a significant improvement of the ORR catalytic activity, as compared with that of leading (naked) commercial Pt/C catalysts. Similar enhancement was observed when Pt/C was modified with the same chlorophenyl groups.

The Pt–ArCl nanoparticles were synthesized by co-reduction of H_2PtCl_4 and 4-chlorophenyl diazonium (see ESI† for details). Chemical modification of commercial Pt/C (Johnson Matthey) was carried out by $NaBH_4$ reduction of Pt/C (80 mg) and 4-chlorophenyl diazonium (0.5 mmol) in an H_2O–THF suspension, and this sample was denoted as Pt/C^{ArCl}.

The morphology of the Pt–ArCl nanoparticles was first characterized by high-resolution transmission electron microscopy, as depicted in Fig. 1. Well-defined lattice fringes with a spacing of 0.23 nm, corresponding to the Pt(111) lattice, can be observed clearly. The average core size of the Pt nanoparticles is estimated to be 1.85 ± 0.28 (inset to Fig. 1), which is significantly smaller than the typical size (~3 nm) of commercial Pt catalysts used in fuel cells.

We then carried out FTIR spectroscopic measurements to further characterize the aryl ligands on the Pt–ArCl nanoparticle surface, as shown in Fig. 2 (a). Two bands at 1565 and 1482 cm^{-1} can be assigned to the aromatic ring skeleton vibrations, and the band at 1092 cm^{-1} to the stretching vibration of C–Cl linked to the aromatic ring. In addition, two weak bands at 3060 and 826 cm^{-1} arise from the C–H stretch in the aromatic ring and out-of-plane C–H deformation vibration (the characteristic peak of *para*-substituted aromatic ring), respectively. The appearance

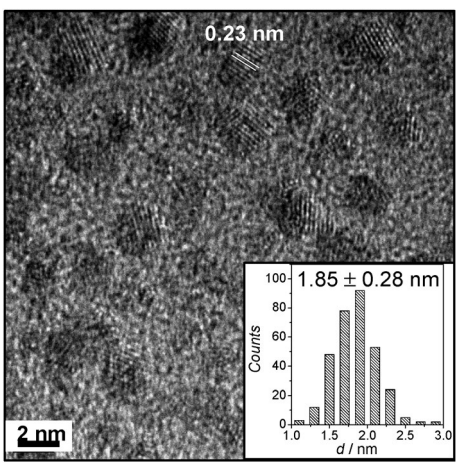

Fig. 1 Representative HRTEM image of the Pt–ArCl nanoparticles. White lines highlight the lattice fringes with a spacing of 0.23 nm for Pt(111). Inset is the nanoparticle core size histogram.

[a] *Department of Chemistry and Biochemistry, University of California, 1156 High Street, Santa Cruz, California 95064, USA. E-mail: shaowei@ucsc.edu*
[b] *State Key Laboratory of Physical Chemistry of Solid Surfaces, Department of Chemistry, Xiamen University, Xiamen 361005, China*
† Electronic supplementary information (ESI) available: Experimental details, additional CV and TGA curves, and TEM images of Pt/C. See DOI: 10.1039/c2cc17945h

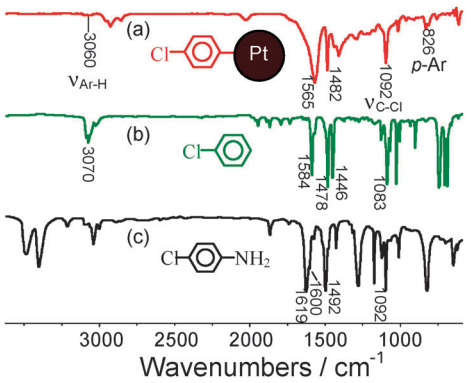

Fig. 2 Transmission FTIR spectra of (a) Pt–ArCl nanoparticles, (b) chlorobenzene, and (c) 4-chloroaniline.

of bands near 2900 cm^{-1} (saturated C–H stretch) indicates that there exists some impurity, which may be due to residual solvents. It is clear that on the Pt–ArCl nanoparticles, the IR band-width of the aromatic ring skeleton vibration at 1565 cm^{-1} is much broader than that of free ligands (1584 cm^{-1} for (b) chlorobenzene, and 1600 cm^{-1} for (c) 4-chloroaniline), and its peak position significantly shifts to a lower wavenumber. These infrared characteristics demonstrate that the chlorophenyl fragments are indeed bound onto the Pt nanoparticles,[16] and there are relatively strong electronic interactions between the aromatic rings and the Pt nanoparticles. Furthermore, thermogravimetric analysis (TGA, Fig. S1 and S2, ESI†) suggests that the aryl ligands likely formed a multilayer structure on the nanoparticle surface.[19,20]

The electrocatalytic activity of the Pt–ArCl nanoparticles for ORR was then evaluated with a rotating ring disk electrode (RRDE) system. The particles were dispersed onto XC-72 carbon black (Pt–ArCl/C, 20 wt% Pt), similar to the commercial Pt/C catalyst that was employed as a benchmark material. The Pt loading on the working electrode (glassy carbon, GC) was 10 μg cm^{-2} in all cases.

Fig. 3a shows the cyclic voltammograms of Pt–ArCl/C, Pt/C and Pt/C^{ArCl} recorded in a N_2-saturated 0.1 M $HClO_4$ solution at a potential scan rate of 100 mV s^{-1}. On the basis of hydrogen adsorption and desorption on Pt (0.05–0.4 V) and Pt loading (2.0 μg), the specific electrochemical surface areas (ECSA) of the Pt–ArCl/C, Pt/C and Pt/C^{ArCl} catalysts were determined to be 96, 80 and 55 m^2 g^{-1}_{Pt}, respectively. The highest ECSA of Pt–ArCl among the three samples was mostly due to the considerably smaller particle size than that of Pt/C

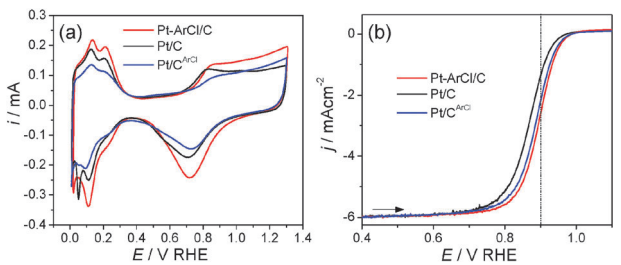

Fig. 3 (a) Cyclic voltammograms, recorded in N_2-saturated 0.1 M $HClO_4$ at 100 mV s^{-1} and (b) forward-scan ORR polarization curves at 10 mV s^{-1}, recorded on a rotating disk electrode in an O_2-saturated 0.1 M $HClO_4$ solution at room temperature of Pt–ArCl/C, commercial Pt/C and chlorophenyl modified Pt/C (Pt/C^{ArCl}) catalysts. Rotation rate: 1600 rpm; Pt loading: 2.0 μg; GC electrode area: 0.20 cm^2.

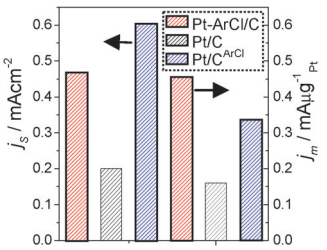

Fig. 4 Comparison of the specific and mass activities at +0.90 V of the Pt–ArCl/C, commercial Pt/C and Pt/C^{ArCl} catalysts.

(3.30 ± 0.42 nm, Fig. S3, ESI†). Note that for Pt/C^{ArCl}, the 30% loss of specific ECSA as compared with that of the "naked" Pt/C was attributed to the blocking of part of the Pt surface sites by the chlorophenyl groups.

Fig. 3b shows the forward-scan ORR polarization curves on a rotating disk electrode at 1600 rpm in an O_2-saturated 0.1 M $HClO_4$ solution at 10 mV s^{-1}. The half-wave potential ($E_{1/2}$) exhibited a positive shift of 28 mV and 20 mV for the chlorophenyl-functionalized Pt–ArCl/C (+0.895 V) and Pt/C^{ArCl} (+0.887 V), respectively, as compared with that of the naked Pt/C catalysts (+0.867 V), signifying the improvement of the electrocatalytic activity by deliberate chemical functionalization. The intrinsic activity (*i.e.*, kinetic current) of the catalysts was further evaluated by the Koutecky–Levich equation in the rotating disk electrode system to correct mass transfer.

The quantitative comparison of the specific activity (j_s, kinetic current normalized by ECSA) and mass activity (j_m, kinetic current normalized by Pt mass) at +0.90 V among the three catalysts is illustrated in Fig. 4. The values of j_s are 0.47, 0.20 and 0.60 mA cm^{-2} on the Pt–ArCl/C, Pt/C and Pt/C^{ArCl} catalysts, respectively; and the corresponding values of j_m are 0.45, 0.16, and 0.33 mA μg^{-1}_{Pt}. As stated above, for naked Pt nanoparticles, the ORR specific activity typically decreases with decreasing particle size.[2,3] Yet, whereas the size of the Pt–ArCl particles is considerably smaller than that of commercial Pt/C (1.85 *vs.* 3.30 nm), the former exhibits 2.3 times higher specific activity. It is worth noting that the mass activity of the Pt–ArCl nanoparticles reported herein has reached the DOE target for 2015 (0.44 mA μg^{-1}_{Pt} at +0.9 V), and it is also superior to most of Pt alloy catalysts reported so far, such as PtPd nanodendrites (0.24 mA μg^{-1}),[21] PtAu (0.2–0.3 mA μg^{-1}),[22] and PtCuCoNi nanotubes (0.19 mA μg^{-1}).[23] This suggests that surface functionalization of Pt nanoparticles may represent an effective route towards the design of improved ORR catalysts.

The enhanced catalytic activity may be correlated with the impeded adsorption of oxygen (*e.g.*, O_{ad} and OH_{ad}) on the Pt surfaces. It has been demonstrated that the reductive desorption of adsorbed oxygen species to form water is the sluggish step during ORR on Pt surfaces, and the deceasing oxygen binding energy by 0.2 eV will optimize the catalytic activity.[1,24] As shown in Fig. 3a, the modification of Pt/C by chlorophenyl groups greatly suppresses the oxygen adsorption on Pt surface. For Pt–ArCl nanoparticles, oxygen adsorption will most likely be impeded by chlorophenyl functionalization, but facilitated by the smaller particle size.[25] As a result, the weakening of oxygen adsorption is not as distinct as that of Pt/C^{ArCl}. To better understand the molecular nature of the improvement of the particle catalytic activity, further studies are

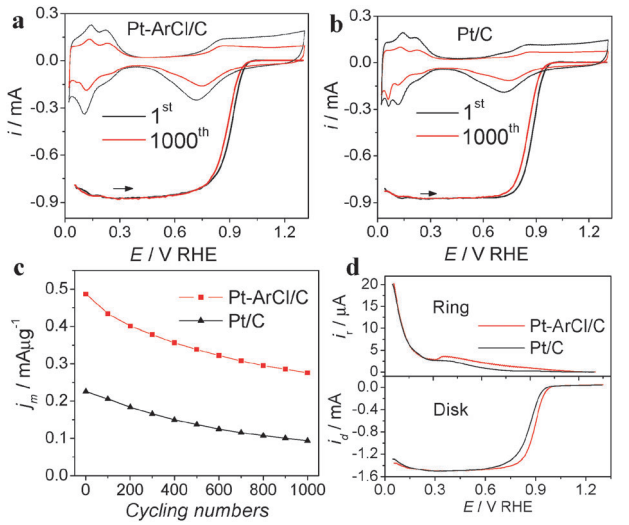

Fig. 5 (a, b) Cyclic voltammograms recorded in a N_2-purged 0.1 M $HClO_4$ solution at 100 mV s^{-1} and ORR polarization curves (50 mV s^{-1}) before and after the durability test. (c) Variation of mass activity with potential cycling numbers. (d) Determination of H_2O_2 produced from ORR on Pt–ArCl/C and Pt/C catalysts by RRDE. Scan rate 10 mV s^{-1}; rotation rate 1600 rpm. The Au ring with a collection efficiency of 0.37 was held at +1.50 V to detect the H_2O_2 intermediate. Note that the ORR polarization curves in (a) and (b) have been corrected for background currents in an O_2-free solution (Fig. S4, ESI†).

needed to elucidate the electronic structures of the Pt–ArCl particles and the interactions between Pt–ArCl and O_2 by, for instance, DFT calculations and/or direct measurements of the d-band center position by ultraviolet photoemission spectroscopy (UPS).[1,24] In addition, studies of the impacts of the electron-withdrawing capability of substituents on ORR will also understand the enhancement mechanism. These will be pursued in future studies.

In addition to catalytic activity, durability is also an important parameter in the evaluation of the performance of ORR electrocatalysts. We used an accelerated protocol to test the durability of the Pt–ArCl and Pt/C nanoparticle catalysts. The test consists of 1000 potential cycles between +0.05 and +1.30 V at a potential scan rate of 50 mV s^{-1} in an O_2-saturated 0.1 M $HClO_4$ solution at a rotating rate of 900 rpm. Note that a relatively high upper potential limit of +1.30 V was used here in order to shorten the test time in comparison with previous studies.[26,27] Fig. 5 (a and b) compares the cyclic voltammograms recorded in a N_2-saturated 0.1 M $HClO_4$ solution, as well as ORR polarization curves for Pt–ArCl and Pt/C catalysts before and after the durability test. After the test, the Pt–ArCl/C and Pt/C exhibited a similar loss in ECSA, *i.e.*, 44% and 43%, respectively. Fig. 5c shows the variation of the mass activity measured at +0.90 V during potential cycling. After 1000 potential cycles, the loss of mass activities at Pt–ArCl/C and Pt/C was 43% and 58%, respectively. It is interesting to note that the mass activity of Pt–ArCl increased from 2.5 to 3.0 times that of Pt/C during these repeated tests, indicating enhanced stability of the Pt–ArCl nanoparticles as compared with that of "naked" Pt/C.

We also measured the yield of H_2O_2 during ORR by RRDE, as shown in Fig. 5d. Based on the ring current generated from the oxidation of H_2O_2, we can see that both Pt–ArCl/C and Pt/C catalysts produced a very low level of H_2O_2. For instance, at +0.40 V, the yield of H_2O_2 was only 1.2% and 0.95% on the Pt–ArCl/C and Pt/C, respectively, corresponding to the numbers of electrons transferred of 3.976 and 3.981.

In summary, stable chlorophenyl-functionalized Pt nanoparticles were synthesized. Because of the high specific surface area and unique surface functionalization, the Pt–ArCl nanoparticles exhibited an ORR mass activity that was up to 2.8 times higher than that of "naked" commercial Pt/C catalysts. The direct modification of commercial Pt/C with chlorophenyl groups also doubled the mass activity, and tripled the specific activity for ORR. Although the exact fundamental mechanism is not clear at this point, the present study suggests that surface functionalization of noble metal nanoparticles by selected organic capping ligands may be a unique and promising route to further improve the electrocatalytic performance in oxygen reduction.

This work was supported by NSF (CHE-1012258). TEM studies were carried out at the National Center for Electron Microscopy, Lawrence Berkeley National Laboratory.

Notes and references

1 V. R. Stamenkovic, B. Fowler, B. S. Mun, G. F. Wang, P. N. Ross, C. A. Lucas and N. M. Markovic, *Science*, 2007, **315**, 493.
2 K. Kinoshita, *J. Electrochem. Soc.*, 1990, **137**, 845.
3 K. J. J. Mayrhofer, B. B. Blizanac, M. Arenz, V. R. Stamenkovic, P. N. Ross and N. M. Markovic, *J. Phys. Chem. B*, 2005, **109**, 14433.
4 R. R. Adzic, J. Zhang, K. Sasaki, M. B. Vukmirovic, M. Shao, J. X. Wang, A. U. Nilekar, M. Mavrikakis, J. A. Valerio and F. Uribe, *Top. Catal.*, 2007, **46**, 249.
5 K. P. Gong, D. Su and R. R. Adzic, *J. Am. Chem. Soc.*, 2010, **132**, 14364.
6 U. A. Paulus, A. Wokaun, G. G. Scherer, T. J. Schmidt, V. Stamenkovic, V. Radmilovic, N. M. Markovic and P. N. Ross, *J. Phys. Chem. B*, 2002, **106**, 4181.
7 Z. M. Peng and H. Yang, *J. Am. Chem. Soc.*, 2009, **131**, 7542.
8 S. Koh and P. Strasser, *J. Am. Chem. Soc.*, 2007, **129**, 12624.
9 J. B. Wu, J. L. Zhang, Z. M. Peng, S. C. Yang, F. T. Wagner and H. Yang, *J. Am. Chem. Soc.*, 2010, **132**, 4984.
10 J. Zhang, H. Z. Yang, J. Y. Fang and S. Z. Zou, *Nano Lett.*, 2010, **10**, 638.
11 B. Genorio, D. Strmcnik, R. Subbaraman, D. Tripkovic, G. Karapetrov, V. R. Stamenkovic, S. Pejovnik and N. M. Markovic, *Nat. Mater.*, 2010, **9**, 998.
12 D. Strmcnik, M. Escudero-Escribano, K. Kodama, V. R. Stamenkovic, A. Cuesta and N. M. Markovic, *Nat. Chem.*, 2010, **2**, 880.
13 Z. Y. Zhou, X. W. Kang, Y. Song and S. W. Chen, *Chem. Commun.*, 2011, **47**, 6075.
14 H. Meng and P. K. Shen, *J. Phys. Chem. B*, 2005, **109**, 22705.
15 F. Mirkhalaf, J. Paprotny and D. J. Schiffrin, *J. Am. Chem. Soc.*, 2006, **128**, 7400.
16 D. Ghosh and S. W. Chen, *J. Mater. Chem.*, 2008, **18**, 755.
17 D. E. Jiang, B. G. Sumpter and S. Dai, *J. Am. Chem. Soc.*, 2006, **128**, 6030.
18 L. Laurentius, S. R. Stoyanov, S. Gusarov, A. Kovalenko, R. B. Du, G. P. Lopinski and M. T. McDermott, *ACS Nano*, 2011, **5**, 4219.
19 A. Adenier, C. Combellas, F. Kanoufi, J. Pinson and F. I. Podvorica, *Chem. Mater.*, 2006, **18**, 2021.
20 J. K. Kariuki and M. T. McDermott, *Langmuir*, 1999, **15**, 6534.
21 B. Lim, M. J. Jiang, P. H. C. Camargo, E. C. Cho, J. Tao, X. M. Lu, Y. M. Zhu and Y. N. Xia, *Science*, 2009, **324**, 1302.
22 K. M. Yeo, S. Choi, R. M. Anisur, J. Kim and I. S. Lee, *Angew. Chem., Int. Ed.*, 2011, **50**, 745.
23 L. F. Liu and E. Pippel, *Angew. Chem., Int. Ed.*, 2011, **50**, 2729.
24 J. Greeley, I. E. L. Stephens, A. S. Bondarenko, T. P. Johansson, H. A. Hansen, T. F. Jaramillo, J. Rossmeisl, I. Chorkendorff and J. K. Norskov, *Nat. Chem.*, 2009, **1**, 552.
25 H. A. Gasteiger, S. S. Kocha, B. Sompalli and F. T. Wagner, *Appl. Catal., B*, 2005, **56**, 9.
26 J. Zhang, K. Sasaki, E. Sutter and R. R. Adzic, *Science*, 2007, **315**, 220.
27 Z. W. Chen, M. Waje, W. Z. Li and Y. S. Yan, *Angew. Chem., Int. Ed.*, 2007, **46**, 4060.